Available online at www.sciencedirect.com
SCIENCE DIRECT®
Polymer 45 (2004) 459–465
polymer
www.elsevier.com/locate/polymer

Electronic properties of heterocyclic aromatic hydroxyl rigid-rod polymers

Y.-H. Tang[a], M.-H. Tsai[a,*], C.C. Wu[b], S.J. Bai[b]

[a]*Department of Physics, National Sun Yat-Sen University Kaohsiung 804, Taiwan, ROC*
[b]*Institute of Materials Science and Engineering, National Sun Yat-Sen University Kaohsiung 804, Taiwan, ROC*

Received 5 August 2003; received in revised form 19 November 2003; accepted 19 November 2003

Abstract

Using first-principles calculations, we find that the electronic structures of PBT, OH-PBT, OH-PBI, and OH-PBI(N) rigid-rod polymers are very different from those of conventional semiconductors. The close agreement between calculated excitation energies and the observed features in the ultraviolet–visible (UV–Vis) absorption spectra enables us to identify that the major features in the UV–Vis absorption spectra are contributed by N 2s to 2p and C 2s to 2p transitions. For OH-PBI(N), the O atom and the substituted N atom also contribute significantly to the threshold of the UV–Vis absorption spectra. The calculated energy bands show significant inter-molecular p_z-orbital coupling perpendicular to the molecular plane.

Keywords: Rigid-rod polymer; PBX; Electronic structure

1. Introduction

Most organic polymers, owing to their long and flexible chain structures, assume random intermolecular orientations in the amorphous state and in solution. However, there is a class of organic polymers, which have more rigid molecular backbones, are called rigid-rod polymers. These rigid-rod polymers tend to aggregate and orient themselves into much more ordered solutions, films and fibers than typical flexible polymers [1–4,7]. Among these rigid-rod polymers, heat-treated polymers like poly{2,6-diimidazo[4,5-*b*:4′5′-*e*] pyridinylene-1,4(2,5-dihydroxy)phenylene} (PIPD) even form a monoclinic three-dimensional crystalline structure [3]. Because of rigidity, these polymers display superior mechanical tenacity and thermo-oxidative stability. The basic rigid-rod system comprises the heterocyclic aromatic polymers of poly(*p*-phenylenebenzazoles) (PBX) as illustrated in Fig. 1 [4,6,7]. PBX constitutes a class of polymers that have a *para*-catenated backbone yielding to a rod like configuration. The only conformational flexibility is provided by the rotation of bonds between alternating phenylene and heterocyclic groups [4,7]. Furthermore, the PBX backbones all have alternating single and double bonds leading to fully conjugated polymers. Because of the conjugated backbone and the collinear and coplanar configuration unique to PBX polymers, investigations are currently centered on the optoelectronic properties of these rigid polymers, mainly for applications as light emitting diodes (LEDs).

The substitution by heteroatoms O, S, and N in PBO (X = O), PBT (X = S), and PBI (X = NH) as shown in Fig. 1 usually give rise to a nonbonding lone-pair electron state (the n state) lying between the bonding, π, and anti-bonding, π^*, states. Most applications of the organic compounds to absorption spectroscopy are based on transition from the n or π to the π^* excited state [8]. These substitutions also cause shifts in the wavelength of the absorption maxima and corresponding changes in the fluorescence peaks. The substitution of oxygen or nitrogen in OH-PBI(N) for the CH group in the benzene ring has also been known to result in a bathochromic shift, i.e. the shift of the fluorescence band toward longer wavelength, and higher band intensity. The addition of the hydroxyl may improve the compression performance and the coplanarity of the molecule. In this study the electronic structure calculations are performed to understand the effects of the substitution of heteroatoms and the addition of the hydroxyl on the light absorption properties of the rigid-rod polymers.

* Corresponding author. Tel.: +886-7-525-3729; fax: +886-7-525-3709.
E-mail address: tsai@mail.phys.nsysu.edu.tw (M.H. Tsai).

0032-3861/$ - see front matter © 2003 Elsevier Ltd. All rights reserved.
doi:10.1016/j.polymer.2003.11.022

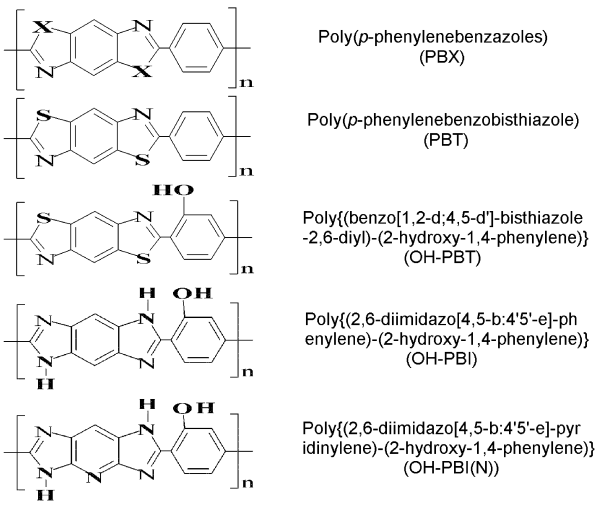

Fig. 1. Structural formula units of PBX, PBT, OH-PBT, OH-PBI, and OH-PBI(N) rigid-rod polymers.

2. Experimental determination of the local order

Since PBT, OH-PBT, OH-PBI and OH-PBI(N) rigid-rod polymers tend to aggregate and orient themselves into much more ordered structures than typical flexible polymers, X-ray diffraction (XRD) measurements can be used to elucidate the local order of these polymers. XRD analyses of the freestanding films of these polymers were carried out at room temperature using a Siemens® D5000 diffractometer with a $\theta-2\theta$ gonimeter. The 2θ angle region was between 1 and 41° in steps of 0.05° and 3 s per step throughout the measurement. Cu Kα radiation ($\lambda = 0.1542$ nm) was extracted from the X-ray tube operated at 1.2 kW (30 mA and 40 kV) using a graphite crystal as the monochromator. XRD spectra obtained for PBT, OH-PBT, OH-PBI, and OH-PBI(N) are shown in Fig. 2(a) and (b). These spectra exhibit distinct features, which show that these polymers have relatively long ranged, though not a macroscopic, local order because the range of order should be much larger than the wavelength of the soft X-ray in order to have distinguished interference peaks. From the positions of the features in the spectra, the inter-molecular distances, a and b, parallel with and perpendicular to the molecular plane, respectively, can be obtained. The inter-molecular distances, a and b, and the length of the structural formula unit, c, are tabulated in Table 1.

The observed a and b are much larger than the widths and thickness of the molecules, which indicates that there are local repulsive forces between edge atoms of adjacent molecules. The a and b are smaller for PBT and OH-PBT than for OH-PBI and OH-PBI(N), which may be due to the rotation of the phenylene in the former that weakens the local repulsive force. The largeness of a and b also indicates that these polymer systems are formed by relatively long ranged van der Waals forces. Since a is smaller than twice the width of the molecules of these polymers, the basic cross sectional units in the ab plane of these polymers contain

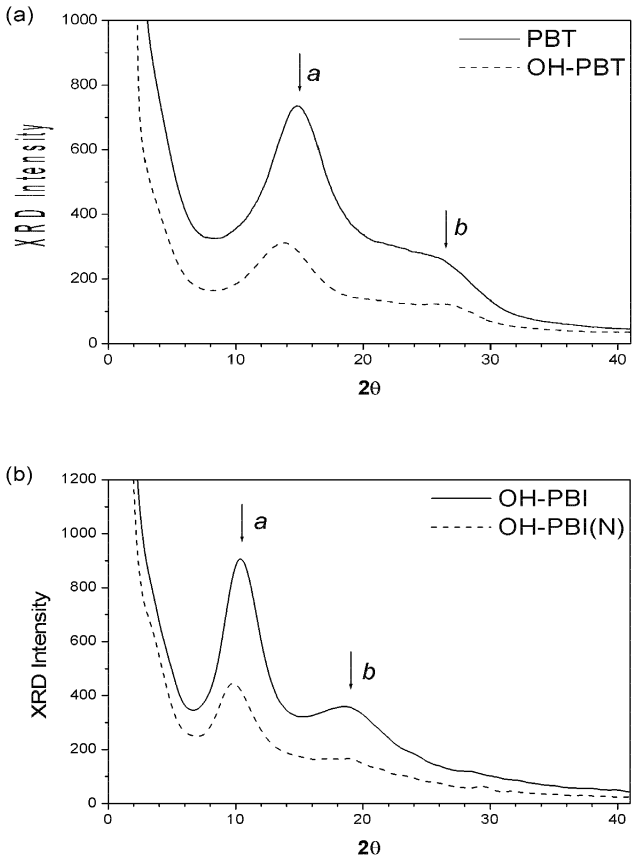

Fig. 2. X-ray diffraction spectra for (a) PBT and OH-PBT and (b) OH-PBI and OH-PBI(N). In these figures a and b are the inter-molecular distances parallel with and perpendicular to the molecular plane, respectively. The length of the structural formula unit, i.e. the periodicity of the polymer chain, c, is behind the direct beam, so that it is not observed.

only one molecular chain. This is different from heat-treated PIPD, in which the basic cross sectional unit, i.e. the base of the unit cell on the ab plane, contains two molecular chains. This difference also indicates that molecular chains in PBT, OH-PBT, OH-PBI and OH-PBI(N) do not aggregate by hydrogen bonds like in PIPD [3,9].

3. The molecular structures

The structural formula units of PBT, OH-PBT, OH-PBI and OH-PBI(N) are shown in Fig. 1. Fig. 3 shows sketches of

Table 1
Lattice constants (a, b, c) used for PBT, OH-PBT, OH-PBI, and OH-PBI(N) in Å

	a	b	c
PBT	5.90	3.60	12.51
OH-PBT	6.44	3.46	12.51
OH-PBI	8.58	4.72	12.24
OH-PBI(N)	9.06	4.77	12.24

the polymer systems, in which a, b, and c periodicities are indicated. The coordinates of the atoms in a structural formula unit are given in Table 2. The coordinates for PBT were obtained by the linked-atom least squares (LALS) method [5] by constraining the bond lengths and bond angles to the values shown in Table V of Ref. [6]. For OH-PBT, the H end of the hydroxyl radical was bended towards the nearby N atom because of the intra-molecular hydrogen bond. The 'ChemOffice 2002' software was used to obtain the atomic coordinates for OH-PBI and OH-PBI(N). Because the sulfur atom is larger than the nitrogen atom, the phenylene rotates about the heterocycle–phenyl bonds in PBT and OH-PBT. When the NH radical substitutes the sulfur atom in OH-PBI and OH-PBI(N), there is almost no rotation of the phenylene. Note the planar heterocycle–phenyl in all the four polymers was chosen to lie in the ac plane.

4. Calculation method

Hageman et al. [9] have used the solid-state calculation method based on the Bloch states of three-dimensional crystalline system to study the electronic structure of heat-treated PIPD. The PIPD system was found to have a monoclinic crystalline structure based on XRD measurement [3]. The present XRD analyses stated previously show that PBT, OH-PBT, OH-PBI and OH-PBI(N) have a local structural order. However, the structural order is not macroscopically long ranged because the features in the spectra are not sharp peaks. Nevertheless, the use of the solid-state calculation method is still adequate because in these polymer systems, the electronic structures are predominantly determined by local bonding. In the present calculation, the inter-molecular distances, a and b, given in Table 1 are used as the periodicities in the x and y directions, respectively, which are perpendicular to the molecular chain. The periodicity, c, along the molecular chain, i.e. along the z-axis, is the length of the structural formula unit of the molecule.

The solid-state calculation method used is the first-principles pseudofunction (PSF) [10] method implemented with the local density approximation (LDA) of Hedin–Lundqvist [11]. The basis wavefunctions in the PSF method are Bloch sums of muffin-tin orbitals, which have spherical Hankel and Neumann tailing functions in the interstitial region augmented with the linearized solutions of the Schrödinger's equation [12] within the muffin-tin sphere of each atom. The pseudofunctions are smooth mathematical functions with the same spherical Hankel and Neumann tailing functions in the interstitial region. The pseudofunctions are expandable by a minimal number of plane waves and are designed to make the calculation of the interstitial and nonspherical parts of the Hamiltonian matrix elements efficiently using the fast Fourier transform (FFT) technique. The muffin-tin radii, R_{MT}, of the C, H, S, N, and O atoms are chosen to be $1.12a_0$, $0.6a_0$, $1.75a_0$, $1.2a_0$, and $1.2a_0$, respectively, based on their covalent radii [13] (a_0 : Bohr radius, $1a_0 = 0.529$ Å).

5. Experimental excitation energies

The ultraviolet–visible (UV–Vis) absorption measurements were performed for the freestanding films of PBT, OH-PBT, OH-PBI and OH-PBI(N) polymers to reveal their excitation energies. The Hitachi® 3500 spectrophotometer was used to obtain UV–Vis transmission spectra [14]. The measurements were performed normal to the freestanding

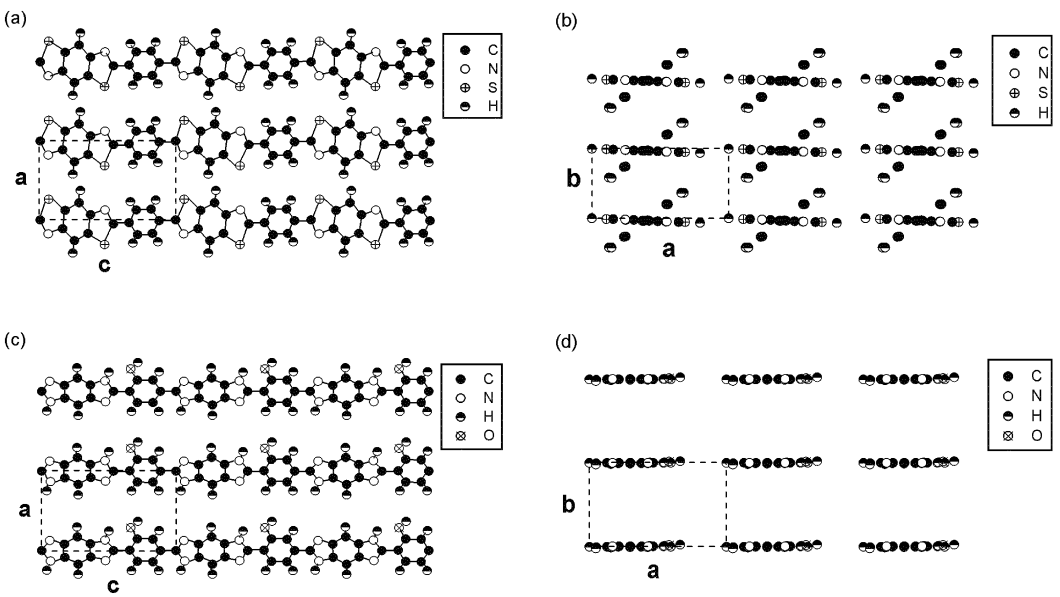

Fig. 3. Representative sketches of the polymer systems considered in this study, which show a, b, and c periodicities. Figures (a) and (b) are for PBT and OH-PBT and (c) and (d) are for OH-PBI and OH-PBI(N).

Table 2
The coordinates of the atoms in a structural formula unit for (a) PBT and OH-PBT and (b) OH-PBI and OH-PBI(N) in Å. The z-axis is along the polymer chain

(a)	PBT			OH-PBT		
	X	*Y*	*Z*	*X*	*Y*	*Z*
C1	0.000	0.000	0.000	0.000	0.000	0.000
C3	−0.663	0.028	2.101	−0.663	0.028	2.101
C4	0.733	−0.041	2.335	0.733	−0.041	2.335
C6	−1.547	0.070	3.170	−1.547	0.070	3.170
C7	−1.013	0.041	4.436	−1.013	0.041	4.436
C8	0.383	−0.028	4.670	0.383	−0.028	4.670
C9	1.269	−0.070	3.603	1.269	−0.070	3.603
C11	−0.283	0.000	6.770	−0.283	0.000	6.770
C13	−0.218	−0.006	8.238	−0.218	−0.006	8.238
C14	−1.091	−0.828	8.996	−1.091	−0.828	8.996
C15	−1.009	−0.816	10.379	−1.009	−0.816	10.379
C16	−0.059	0.017	11.006	−0.059	0.017	11.006
C17	0.816	0.841	10.260	0.816	0.841	10.260
C18	0.744	0.836	8.885	0.744	0.836	8.885
N2	−1.034	0.050	0.767	−1.034	0.050	0.767
N12	0.753	−0.049	6.004	0.753	−0.049	6.004
S5	1.556	−0.078	0.808	1.556	−0.078	0.808
S10	−1.837	0.079	5.963	−1.837	0.079	5.963
H20	−2.472	0.116	3.033	−2.472	0.116	3.033
H21	2.194	−0.116	3.742	2.194	−0.116	3.742
H22	−1.725	−1.384	8.567	−1.725	−1.384	8.567
H23	−1.620	−1.391	10.876	−1.620	−1.391	10.876
H24	1.506	1.445	10.706	1.506	1.445	10.706
H25	1.379	1.435	8.327	1.490	1.189	7.417
O19				1.706	1.679	8.238
(b)	OH-PBI			OH-PBI(N)		
	X	*Y*	*Z*	*X*	*Y*	*Z*
C1	0.000	0.000	0.000	0.000	0.000	0.000
C3	−0.727	0.023	2.117	−0.728	0.008	2.138
C4	0.687	0.023	2.064	0.687	0.005	2.056
C6/N6	−1.458	0.032	3.309	−1.418	0.011	3.297
C7	−0.687	0.041	4.478	−0.673	0.013	4.417
C8	0.728	0.043	4.424	0.747	0.018	4.392
C9	1.459	0.035	3.232	1.482	0.011	3.209
C11	0.002	0.046	6.544	−0.002	0.027	6.500
C13	0.027	0.037	8.014	0.005	0.033	7.970
C14	−1.184	−0.007	8.723	−1.210	−0.076	8.665
C15	−1.198	−0.029	10.118	−1.238	−0.083	10.060
C16	0.006	−0.005	10.816	−0.047	0.030	10.771
C17	1.210	0.043	10.113	1.160	0.144	10.082
C18	1.249	0.064	8.716	1.215	0.142	8.685
N2	1.090	0.009	0.738	1.090	−0.001	0.728
N5	−1.124	0.008	0.789	−1.113	0.006	0.813
N10	1.124	0.049	5.752	1.127	0.030	5.728
N12	−1.094	0.043	5.801	−1.090	0.013	5.737
H20	−2.113	0.003	0.449	−2.104	0.008	0.478
H21	−2.557	0.029	3.326	2.580	0.010	3.185
H22	2.558	0.033	3.215	2.105	0.039	6.095
H23	2.107	0.050	6.105	−2.164	−0.169	8.123
H24	−2.149	−0.031	8.192	−2.189	−0.180	10.608
H25	−2.146	−0.068	10.675	2.088	0.239	10.668
H26	2.149	0.064	10.688	3.096	0.372	8.756
H27	3.143	0.141	8.769			
O19	2.454	0.111	8.085	2.421	0.265	8.067

films in ambient conditions covering an energy range from 1.55 to 6.7 eV at a scanning rate of 0.5 eV/min using a photomultiplier as the detector. The transmission value was converted using the Beer's law to the optical absorbance $-(\ln T) \equiv \tilde{A}t$, where $\tilde{A}$ is the attenuation coefficient and t is the film thickness.

6. Calculated electronic structures

The calculated energy bands of PBT, OH-PBT, OH-PBI, and OH-PBI(N) polymers along five directions in the first Brillouin zone are shown in Fig. 4(a)–(d). In these figures, the zero energy is chosen to be the Fermi level, E_F, which is the highest occupied level. In these figures Γ, M, X, N, and Y represent the Brillouin zone center, $((\pi/a),(\pi/b),0)$, $((\pi/a),0,0)$, $((\pi/a),(\pi/b),(\pi/c))$, and, $(0,(\pi/b),0)$ points, respectively. Along ΓM, ΓN, and ΓY directions, the large dispersion of energy bands shows significant inter-molecular p_z-orbital coupling perpendicular to the molecular plane. The very small dispersion of energy bands along the ΓX direction shows no significant inter-molecular coupling parallel with the molecular plane. The energy bands of PBT and OH-PBT, which have a large dispersion, are dominantly contributed by the 2p orbitals of the C atoms at the edge of phenylene. For OH-PBI and OH-PBI(N), the energy bands near E_F even have a larger dispersion, which are due to the couplings of enlarged negatively charged O atoms in adjacent molecules. Note that the ionic radius of O^- is 1.76 Å [13], and the atomic radius of the neutral O atom is 0.73 Å [13].

The UV–Vis absorption spectra and the calculated PDOSs for PBT, OH-PBT, OH-PBI, and OH-PBI(N) are shown in Fig. 5(a)–(d) and Fig. 6(a)–(d), respectively.

These PDOSs show that the electronic structures of these polymers are very different from those of semiconductors/insulators. In the latter, the energy states near E_F, i.e. the valence band maximum (VBM), are contributed by anion p orbitals, while those states near the conduction band minimum (CBM) are contributed by cation s orbitals. The optical transition from VBM to CBM is allowed because it obeys the dipole transition rule of light absorption that requires a change of angular momentum quantum number by 1. Thus, in semiconductors/insulators, photon absorption has a threshold corresponding to the energy gap. However, for PBT, OH-PBT, OH-PBI, and OH-PBI(N) polymers, the calculated band structures show that their lowest unoccupied energy states, which correspond to CBM in semiconductors/insulators, are not s-like states, so that the photon absorption transition from highest occupied states to lowest unoccupied states are forbidden by the dipole transition rule. Thus, the photon absorption threshold cannot be interpreted as the energy gap in these polymers. Thus, details of PDOSs are needed to understand the observed UV–Vis absorption spectra.

The dipole transition rule for photon absorption requires transitions from the occupied s-PDOS to the unoccupied

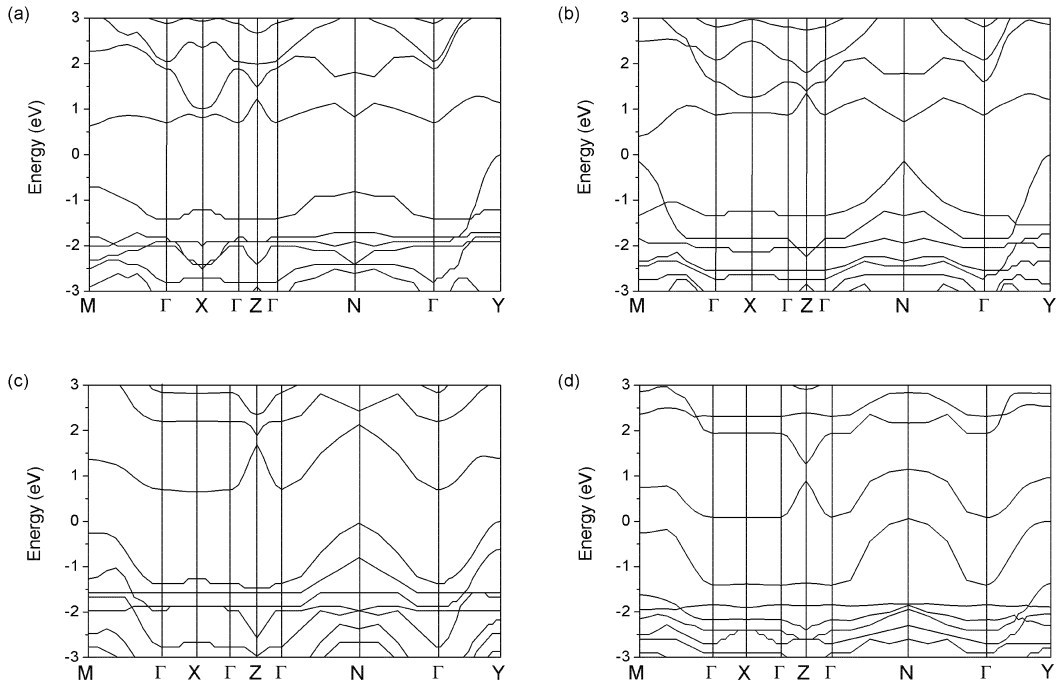

Fig. 4. The calculated band structures for (a) PBT, (b) OH-PBT, (c) OH-PBI, and (d) OH-PBI(N). Γ, M, X, Z, N, and Y represent the Brillouin zone center, $((\pi/a),(\pi/b),0)$, $((\pi/a),0,0)$, $(0,0,(\pi/c))$, $((\pi/a),(\pi/b),(\pi/c))$, and $(0,(\pi/b),0)$ points, respectively.

p-PDOS or from the occupied p-PDOS to the unoccupied s-PDOS. Because there is almost no unoccupied s-PDOSs within 5 eV above E_F, only transitions from the occupied s-PDOS to the unoccupied p-PDOS will be discussed. From the comparison between the features in the UV–Vis absorption spectra and the calculated PDOSs, the transitions that contribute to the observed features in the UV–Vis absorption spectra can be identified.

In the UV–Vis absorption spectra of PBT and OH-PBT shown in Fig. 5(a) and (b), the first feature located at 2.7 ± 0.3 eV can be attributed to the N-2s to N-2p transition because the calculated energy separation is about 3.0 eV as

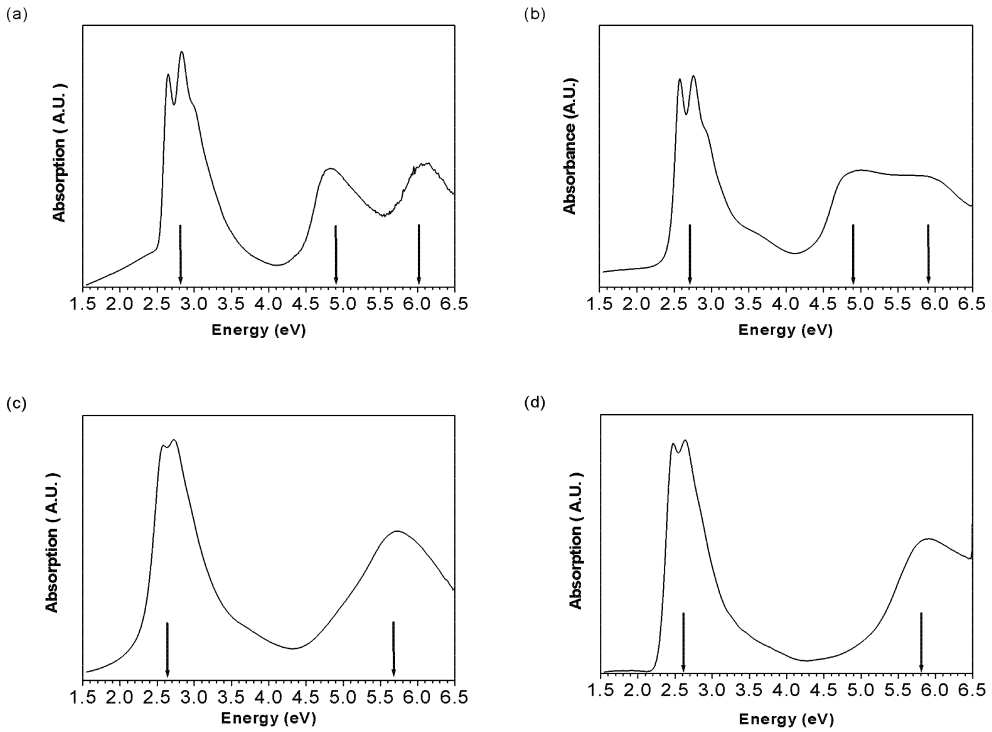

Fig. 5. The UV–Vis absorption spectra for (a) PBT, (b) OH-PBT, (c) OH-PBI, and (d) OH-PBI(N).

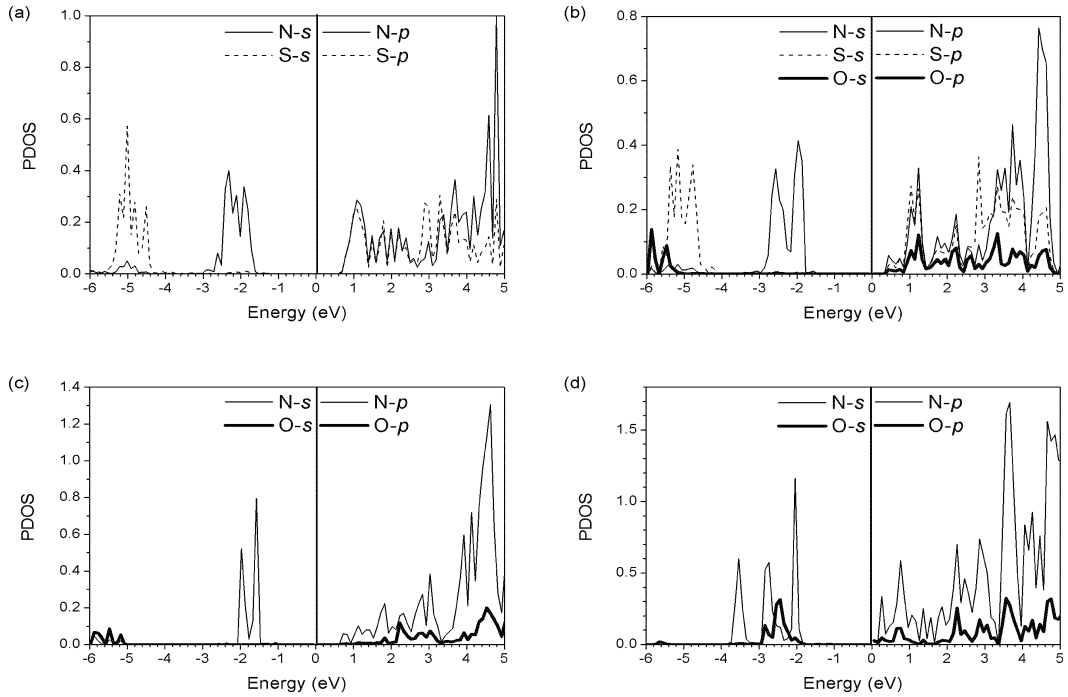

Fig. 6. The calculated partial densities of states (PDOS's) for (a) PBT, (b) OH-PBT, (c) OH-PBI, and (d) OH-PBI(N).

can be seen in Fig. 6(a) and (b). The second feature located at 4.9 ± 0.3 eV also can be attributed to the N-2s to N-2p transition with a calculated energy separation of about 5.0 eV. The third feature located at about 5.9 ± 0.5 eV can be attributed to the S-3s to S-3p transition with a calculated energy separation of about 5.9 eV. The O-2s to O-2p transition also contributes to the third feature for OH-PBT with a calculated energy separation of about 6.0 eV. In the UV–Vis absorption spectra of OH-PBI and OH-PBI(N) shown in Fig. 5(c) and (d), the first feature located at 2.6 ± 0.3 eV can be attributed to the N-2s to N-2p transition at the N atoms that are not bonded with the H atom. The calculated energy separations between these N orbitals as shown in Fig. 6(c) and (d) are about 2.8 eV. The O-2s to O-2p transition also contributed to this feature for OH-PBI(N). The second feature located at 5.7 ± 0.6 eV can be attributed to the C-2s to C-2p transition with a calculated energy separation of about 5.8 eV. The close agreement between calculated energy separations and observed UV–Vis absorption features indicates that calculated electronic structures based on a three-dimensional periodic structural model represent well those of PBT, OH-PBT, OH-PBI, and OH-PBI(N) polymers, although these polymers do not have a long-ranged periodicity.

The s-derived features of the two N atoms in PBT are located at the same energy range between −3 and −1 eV due to the conjugate symmetry as shown in Fig. 7(a), so are those of the two S atoms. However, the N atom, N12, in OH-PBT benefits from forming an intra-molecular hydrogen bond with the H atom in the hydroxyl because its electrons see the attractive potential of the positively charged H atom. Thus the s-derived features of N12 drop down to lower energies as shown in Fig. 7(b). The s-derived features of the S atom, S10, also drop down in energy due to the formation of an inter-molecular hydrogen bond with the H atom in the hydroxyl of an adjacent molecule. The N atom, N2, in OH-PBI and OH-PBI(N) benefits from forming an intra-molecular hydrogen bond with the H atom in the hydroxyl, so that its s-derived features drop down in energy as shown in Fig. 7(c) and (d). Due to the larger separation between molecules, i.e. *a*, the N atom, N12, however, forms a quite weakened inter-molecular hydrogen bond with the H atom in the NH radical of the adjacent molecule, so that its s-derived features remain in the similar energy range between −4.0 and −1.5 eV. The s-derived features of N5 and N10 in the two NH radicals are deep in energy due to the N–H bonding, so that they do not contribute to the UV–Vis absorption spectrum. OH-PBI(N) has an additional N atom, N6, which forms a quit weakened inter-molecular hydrogen bond with H atom in the CH group of the adjacent molecule, has s-derived features in the similar energy range as that of N12 and contributes to the threshold of the UV–Vis absorption spectrum shown by the dotted line.

The calculated PDOSs of these four polymers show trends of the influence of the substitutes. First, the features in the occupied s-PDOSs of N atoms, which are not bonded to the H atoms, are located between 1.5 and 4 eV below E_F.These N 2s states contribute dominantly to the threshold in the UV–Vis absorption spectra. However, the features of the occupied s-PDOSs of those N atoms, which are bonded to the H atoms, are located at deeper energies. Second, the features in the occupied s-PDOSs of S atoms are located between 4 and 6 eV below E_F for PBT and OH-PBT. Third, for OH-PBT and OH-PBI, the hydroxyl derivatives of PBT

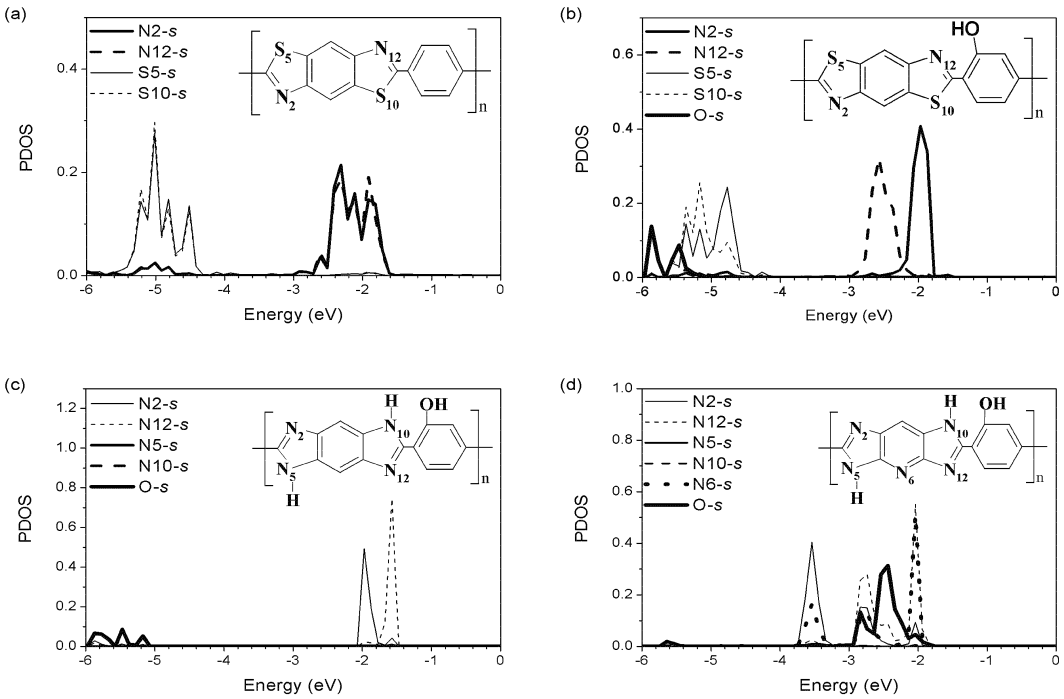

Fig. 7. The calculated s-derived partial densities of states (PDOSs) of the individual atoms for (a) PBT, (b) OH-PBT, (c) OH-PBI, and (d) OH-PBI(N).

and PBI, the features in the occupied s-PDOSs of O atoms are located at about 6 eV below E_F. In contrast, when the CH group in the middle benzene ring of the heterocycle–phenyl is replaced by N in OH-PBI(N), the feature in the occupied O s-PDOSs moves to the higher energy between 2 and 3 eV below E_F. Therefore, substitution with suitable radicals can shift s-PDOSs to within the absorption or emission energy range of visible light, which can be utilized to modulate the frequency of the LED.

7. Conclusion

The good agreement between the UV–Vis absorption spectra and our calculated excitation energies show that the solid-state calculation method is applicable to the polymer systems. Our band structure results show significant inter-molecular p_z-orbital coupling perpendicular to the molecular plane and insignificant inter-molecular coupling parallel with the molecular plane. N and C atoms are found to contribute dominantly to the leading features in the UV–Vis absorption spectra of these polymers. In contrast, the N atoms in the NH radical have no contribution to the UV–Vis absorption spectra for OH-PBI and OH-PBI(N). S atoms are also found to contribute to the higher-energy features in the UV–Vis absorption spectra of PBT and OH-PBT.

Acknowledgements

C.C Wu and S.J. Bai wish to thank the National Science Council of R.O.C. for their support (Contract No. NSC-92-ET-7-110-004-ET).

References

[1] Jenkins S, Jacob KI, Polk MB, Kumar S, Dang TD, Arnold FE. Macromolecules 2000;33:8731.
[2] Tomlin DW, Fratini AV, Hunsaker M, Wade Adams W. Polymer 2000;41:9003.
[3] Klop EA, Lammers M. Polymer 1998;39:5987.
[4] Welsh WJ, Bhaumik D, Mark JE. Macromolecules 1981;14:947.
[5] Fratini AV, Cross EM, O'Brien JF, Adams WW. Polymer 1981;27:861.
[6] Fratini AV, Lenhert PG, Resech TY, Wade Adams W. Mater Res Soc Symp Proc 1989;134:431.
[7] Wellman MW, Wade Adams W, Wolff RA, Wiff DR, Fratini AV. Macromolecules 1981;14:935.
[8] Krasovitskii BM, Bolotin BM. Organic luminescent materials. Weinheim: VCH Press; 1988. Translated by Vopian VG.
[9] Hageman JCL, van der Horst JW, de Groot RA. Polymer 1999;40:1313.
[10] Kasowski RV, Tsai MH, Rhodin TN, Chambliss DD. Phys Rev B 1986;34:2656.
[11] Hedin L, Lundqvist BI. J Phys C 1971;4:2064.
[12] Andersen OK. Phys Rev B 1976;12:3060.
[13] Table of periodic properties of the elements. Sargent-Welch Scientific Company, Skokie, IL; 1980.
[14] Bai SJ, Wu CC, Tu LW, Lee KH. J Polym Sci PartB: Polym Phys 2002;40:1760.